Journal of Materials Science and Engineering A 10 (3-4) (2020) 53-59
doi: 10.17265/2161-6213/2020.3-4.002

Electrical Conductivity Behavior of the Aluminum Alloy 2024 during Artificial Aging

Daniel Diehl, Carlos Köhler, Eduardo Luis Schneider and Thomas Gabriel Rosauro Clarke
Federal University of Rio Grande do Sul, Porto Alegre 15.090, Brazil

Abstract: Precipitation-hardened aluminum alloys need to be heat treated to achieve the mechanical properties required for their application. The production of these materials can be optimized to make them more attractive and competitive comparing to other materials such as composites that have a growing and large market share in aeronautics field. One way to do this is by controlling the artificial aging of precipitation-hardenable aluminum alloys, such as the 2000 series Al-Cu alloys. These alloys can be monitored in real time by analyzing their conductivity behavior inside the furnace. The objective of this work is to evaluate the electrical conductivity behavior in real time of the 2024 alloy during the artificial aging at 190 °C. For this, analyses were made in order to assess the behavior of the microhardness curve by aging time and its microstructural characterization with thermal treatments in the times of 1 h to 9 h interrupted every 1 h. The results of the electrical conductivity versus hardness curve showed a significant correlation and indicate that this measure has great potential to be used as a tool to control the thermal treatment of aging.

Key words: Fur-terminal method, heat treatment, age hardening, precipitation, aluminum alloys, aluminum 2024.

1. Introduction

Aluminum manufacturers for the aeronautical industry have invested in technology in order to make their product more competitive in the market compared to composite materials by improving the properties of aluminum and the quality of its production [1-3]. Al-Cu alloys of the 2000 series have their application in aircraft structures, mainly in the wings, as they present the excellent mechanical resistance obtained by heat treatment accompanied by good toughness [4-6].

The present work aims to evaluate the behavior of the electrical conductivity during the heat treatment of artificial aging in a 2024 alloy, thus, to show the relationship between the hardness and electrical conductivity of this alloy. In this way, the time of the heat treatment can be optimized, as well as the quality control of the material during the process. The analysis of electrical conductivity was performed in real time using the four-terminal method during the heat treatment process and a correlation between hardness and aging times was stablished. This method is used in electronics to analyze the electrical resistivity of metallic materials [7-9], but it is little explored to monitor the behavior of electrical conductivity during artificial aging. During the monitoring and characterization of the 2024 alloy, analyses of hardness, electrical conductivity and material image were performed from samples as received, solubilized at 495 °C for 3 h, and with artificial aging treatment. The artificial ageing was interrupted at intervals of 1 h with a total time of 9 h at 190 °C.

The 2024 aluminum alloy belongs to the 2xxx series, which can be divided into two main groups: the Al-Cu alloys with relatively low magnesium content and the alloys with relatively high magnesium content, above 1%, also called Al-Cu-Mg. In the first group, precipitation hardening is related to the precursor phases of the Al_2Cu phase, while in the second group, the hardening is related to the S' Al_2CuMg phase [5, 6, 10-14].

The copper content influences the continuous increase in hardness due to the formation of

Corresponding author: Daniel Diehl, master student, metallurgical engineer, research field: material science.

precipitates that consist of a cluster of solute and solvent atoms. The Guinier-Preston zone formed in the matrix due to the high concentration of copper maintains coherence with the matrix and constitutes an obstacle to the movement of dislocations more effectively than the solute atoms in their individual form, even when the interaction energy with dislocations associated with the atoms in the solid solution is high. These GP zones are also formed in artificial aging, being considered a precursor to metastable intermediate precipitates [10, 12-14].

The magnesium content of the 2024 alloy in the solid solution accelerates natural aging and during artificial aging refines the θ' phases, increasing its density and improving its mechanical strength. The immobilized clusters then serve as nuclei for the formation of θ' precipitates. The continuation of the heat treatment leads to the formation of a thermodynamic equilibrium precipitate θ' having Al_2Cu chemical composition, in which, even if the treatment continues, there is no change in its characteristics, except for the size, which tends to coalesce, decreasing the hardness when compared with the coexistence interval of phases θ'' and θ' [10, 12-14].

The hardening of aluminum alloys by heat treatment is a three-step process: solubilization, tempering and artificial aging. For the precipitation hardening reaction it is necessary initially to produce a solid solution. The process by which this is done is called solubilization heat treatment and results in the solid solution of the maximum amounts of the soluble hardening elements in the alloy. This process consists of raising the temperature in the alloy for a certain time to obtain an almost homogeneous solid solution. The thermal treatment of artificial aging for the gain of mechanical resistance involves the critical control of heating in the treatment and cooling range, thus resulting in the desired microstructure. The behavior of the hardness during the heat treatment period of artificial aging at 190 °C shows a rapid increase in the first hours, which is possibly caused by the formation of the GPB zones. After this, the hardness increases at lower rates possibly due to the formation of intermediate phases: in the condition of maximum strength both the θ and θ' transition precipitates may be present [10-12].

Electrical conductivity in metals is associated with changes in the scattering of conduction electrons and by network vibration [8, 15-18]. In general, this influence is related to imperfections in the crystalline network that act as spreading centers and can be treated as stationary, in the case in question, because the impurities represent local disturbances in the crystalline network. In 2024 alloy, the Young's modulus is affected depending on the process or heat treatment and, with this the spectrum of the network vibration is modified. Regarding the solid solution condition found in the 2024 alloy, the addition of the copper alloy element promotes a decrease in conductivity due to the increase in electron dispersion, despite the fact that copper has greater electrical conductivity than aluminum [16].

The four-terminal method technique is used in other scientific works [7-9] to analyze the behavior of electrical resistivity. The technique is used in equipment such as ohmmeters for measuring resistance of metallic materials up to the order of 1 mΩ [17]. The principle of the technique for the experiment is based on the electrical resistance between any two points of the metallic material, applying a potential difference between these points with a known electrical current.

The solubilized condition of the 2024 alloy has high electron dispersion caused by vacancies, by alloy atoms present in the matrix and by the formation of the GP and GPB zones with dimensions comparable to the electron wavelength; in addition, distortions and displacements in the contours of these zones or in their clusters also increase electro scattering [15]. Electrical conductivity varies with two simultaneous processes: there is a decrease in the number of

vacancies and a cluster of Cu and Mg. During the initial minutes of heat treatment, these processes tend to increase the electrical conductivity due to the increase in the purity of the matrix, but simultaneously there is a significant decrease in the electrical conductivity due to the appearance of newly formed precipitates, which are small enough to be effective, as electron dispersers [15]. After the first hour of artificial aging, larger precipitates are formed, which are not good electron dispersers, thus resulting in a decrease in electrical conductivity, but not in the final amount.

2. Materials and Methods

In all samples, the solubilization heat treatment was carried out at 490 °C for 3 h in a muffle furnace and cooled in water at 60 °C to avoid cracks and defects. Micrography and hardness analyses were performed on the samples as received and as well with heat treatment of solubilization and with heat treatment of artificial aging at 190 °C interrupted with an interval of 1 h, 2 h, 3 h, 4 h, 5 h, 6 h, 7 h, 8 h, 9 h. The real-time monitoring of the samples for analysis of relative electrical conductivity was carried out continuously inside the furnace.

The chemical composition of three samples with dimensions of Ø2 cm × 3 mm was analyzed in an optical emission spectrometry equipment model Q2 ION.

For these analyses, eleven samples were sanded and later polished in three steps with diamond paste with particle size of 4 μm, 1 μm and 0.5 μm in each step. In optical microscopy the samples were etched with Keller reagent and a Hitachi electron emission microscopy-11th operating up to 100 KV was employed.

The microhardness analysis was performed with samples prepared with dimensions of 1 cm × 1 cm × 3 mm. The microdurometer applied a load of 0.3 for 20 s.

The experiment consisted of the material electrical conductivity analysis inside the furnace during the thermal treatment at 190 °C. The four point method consists of applying a voltage at the sample ends to reach an electrical current of 2 A. This current I is measured by a multimeter in series with the circuit and the measurement of the electrical voltage is performed by another multimeter at points V_1 and V_2, as shown in Fig. 1. Three samples were prepared in dimensions of 4 mm^2 × 18 cm for this experiment.

In this experiment, a direct current source and two multimeters were used. The measurement uncertainty was 0.7 %, as determined by statistical analysis. The configuration of the experiment is shown in Fig. 2.

The electrical conductivity σ was calculated from the relationship of the first-Ohm's law and second-Ohm's law. The resistance of the material is found by Eq. (1), given by Ohm's law:

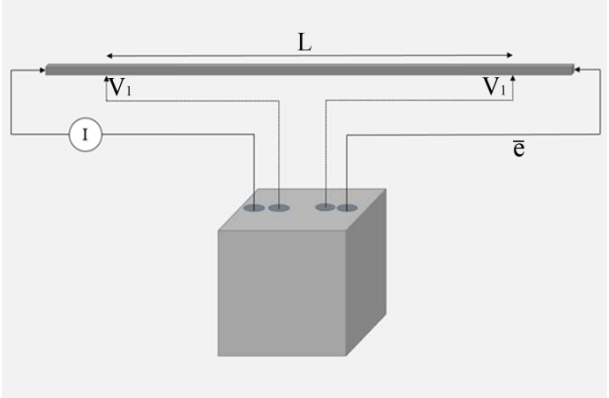

Fig. 1 Design of the four-terminal method experiment model.

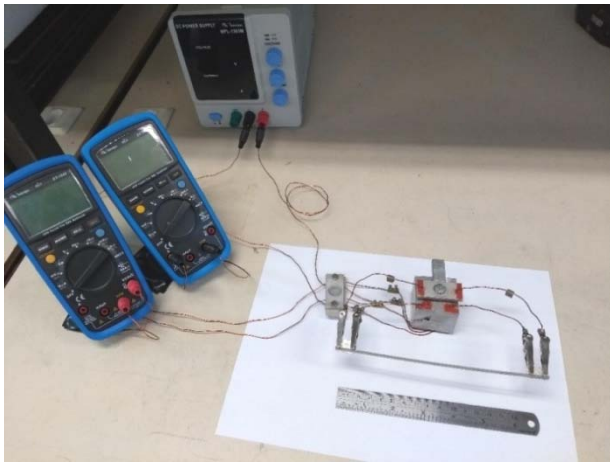

Fig. 2 Assembly of the four-terminal method experiment.

$$R = U/I \ [\Omega] \quad (1)$$

where R is the material resistance, U the applied voltage V and I the electrical current A. The electrical resistivity ρ is given according to Ohm's law, where A is the section area and L is the sample length, shown in Eq. (2).

$$\rho = R * A/L \ [\Omega/m] \quad (2)$$

3. Results and Discussion

The chemical composition of the 2024 alloy is shown in Table 1 [19, 20]. The ratio between %Cu and %Mg greater than 1.5 provides the information that the formation of the S phase will be favored; in alloy 2024 this ratio varies between 2.11 and 4.08.

The composition analysis by optical emission spectrometry analysis is shown in Table 1. The result shows that the chemical composition is within the limits of the range that classifies the 2024 alloy [20].

The ratio found between %Cu and %Mg is 2.88, which favors the greater formation of the hardening phase Al_2CuMg over the phase Al_2Cu. The 0.158% iron content provides the formation of unwanted phases such as inclusions and dispersoid phases, which do not provide a significant hardness gain [3, 10].

The result by scanning electron microscopy in the sample as received is shown in Fig. 3. From the obtained image, an analysis was performed by dispersive energy spectroscopy (EDS) on the particles found. The presence of the Al_2CuMg and Al_2Cu phases was verified in Fig. 3 and shows identification of regions such as A, B, C and point D. The relationship found between Cu and Mg in the result of the chemical composition favors the formation of the S phase, however point D of Fig. 3 shows the probable formation of the Al_2Cu phase, shown as a rounded white precipitate [11, 21, 22].

Table 1 Chemical composition (% wt).

	Cu	Mg	Mn	Fe	Si	Zn
2024	3.8-4.9	1.2-1.8	0.3-0.9	0.5	0.5	0.25
Sample	4.1	1.4	0.7	0.2	0.1	0.06

The result of the EDS performed in the sample matrix as received has a uniform distribution of the precipitated points, indicating a significant presence of its elements with greater content in the 2024 sample. In Fig. 3, a few white dots and many regions with uniform black dots in the matrix are observed, being possible that these dark regions are the detachment or dissociation of precipitates during polishing.

Fig. 4 shows the variation in the hardness of the 2024 aluminum alloy as a function of the artificial aging time. The evolution of microhardness in the time interval of up to 9 h can be plotted with a curve with one or more peaks [21, 23]; a characteristic peak was seen in 8 h.

The hardening curve of the aluminum alloy 2024 reveals that its mechanical strength increases gradually according to the artificial aging process. In the first hour of heat treatment the hardness increased rapidly, as is also observed in the work of Banhart [8], given an increase in the formation of the Al_2CuMg phase. The variation in hardness as a function of the artificial aging time showed a decrease in hardness in 2 h. After 3 h the increase in hardness is more subtle and may be associated with the intermediate phases of Al_2Cu and Al_2CuMg. The maximum hardness found in the hardness behavior in relation to the artificial aging time at 190 °C was 153 HV, reached in 8 h of heat treatment. The hardness of the material received and the behavior during heat treatment are within the limit specified [20].

The result of the experiment using the four-terminal method is shown in Fig. 4. The figure shows the behavior of the electrical conductivity curve as a function of the heat treatment time of artificial aging at 190 °C. The analysis of this aging treatment in real time revealed an interesting aspect about the resulting curve and the hardness curve. The variation in the electrical conductivity of the 2024 alloy during aging at 190 °C is related to the way in which Cu and Mg elements are organized in the microstructure and how it affects the electro-scattering. While in the first hour

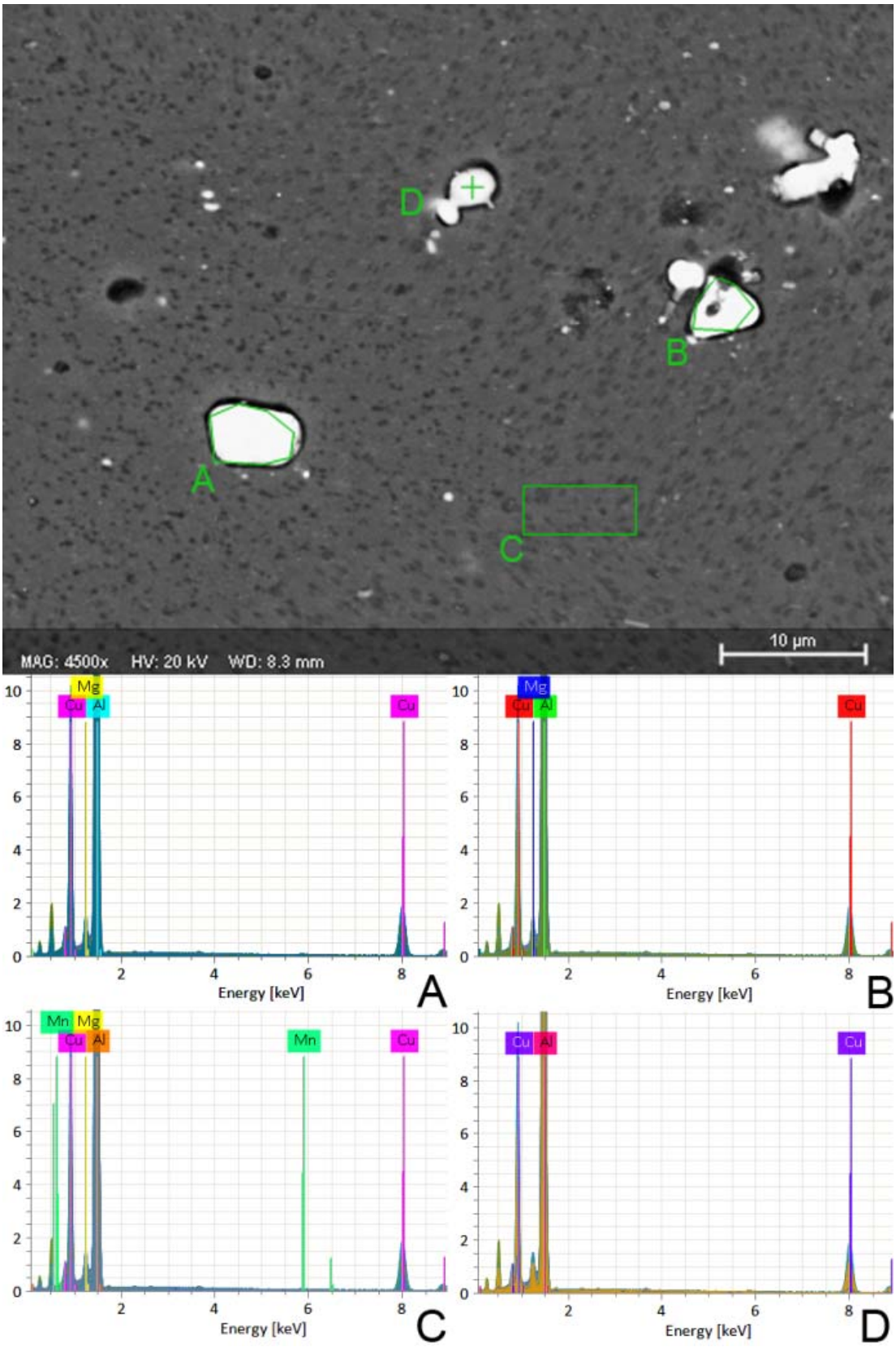

Fig. 3 Scanning electron microscopy image on alloy 2024 with analysis by EDS in the matrix (region C) with fine precipitates and, in the clear regions, the presence of the phases Al_2CuMg (regions A and B) and Al_2Cu (point D).

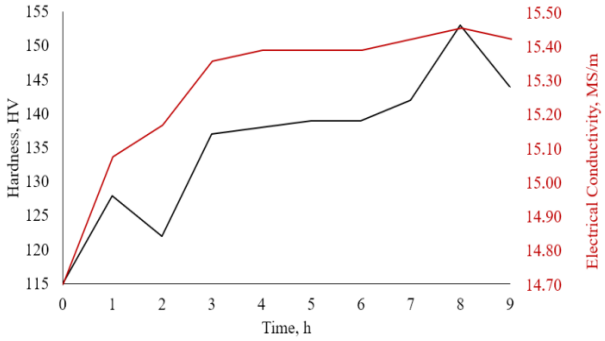

Fig. 4 Behavior of electrical conductivity in real time and the relationship with its hardness.

of heat treatment a pronounced increase in electrical conductivity is observed, in the following hours there is a decrease in the gradient, this behavior being probably linked to the loss of solute caused by formation of precipitates. The electrical conductivity increases rapidly with the decrease of copper in solution [15, 18]. However, this increase becomes smaller and smaller with lower levels of copper in solution, which is caused by the diffusion mechanisms and also by the increase in precipitates that contribute to electro-scattering [24].

In addition, the behavior of the electrical conductivity is disturbed by the temperature: the disturbance in the crystalline network is observed by the higher values on the y-axis of the electrical conductivity curve shown in Fig. 4.

The presence of a peak in Fig. 4 corresponds to a precipitation stage also found in the hardness curve. This allows the progress of aging and the precipitation sequence to be evaluated with measurements of electrical conductivity. This shows that electrical conductivity is able to monitor heat treatment in real time. The study of the behavior of electrical conductivity during heat treatment enables the understanding and better control of mechanical properties. This can have practical purposes, such as time optimization, quality control, and efficiency and even automation of heat treatment.

4. Conclusions

The samples aged thermally at 190 °C showed the values of hardness and electrical conductivity that are quite dependent on the aging conditions, and the combination of these can allow the verification of the evolution of the artificial aging process over time. The value of electrical conductivity is derived from its high sensitivity to microstructural parameters that affect electro scattering. The electrical conductivity behavior related to the hardness curve offers a good tool for process control and the study of the electrical behavior of the 2024 alloy during real-time artificial aging heat treatment, due to the practicality of the measurements.

References

[1] Brough, D., and Jouhara, H. 2020. "The Aluminum Industry: A Review on State-of-the-Art Technologies, Environmental Impacts and Possibilities for Waste Heat Recovery." *Int. J. Thermofluids* 1-2 (2): 100007.

[2] Rambabu, P., Prasad, N. E., and Wanhill, R. J. H. 2016. *Aluminum Alloys for Aerospace Applications, Aerospace Materials and Material Technology*, edited by Prasad, N. E., and Wanhill, R. J. H. Singapore: Springer.

[3] Starke, E. A., and Staleyt, J. T. 1996. "Application of Modern Aluminum Alloys to Aircraft." *Prog. Aerosp. Sci.* 32: 131-72.

[4] Li, G., Lu, H., Hu, X., Lin, F., Li, X., and Zhu, Q. 2020. "Current Progress in Rheoforming of Wrought Aluminum Alloys: A Review." *Metals* 10 (2): 238.

[5] MacKenzie, D. S. 2018. "Heat Treatment Practice of Wrought Age-Hardenable Aluminum Alloys." *Alum. Sci. Technol* 2A (11): 462-77.

[6] Hong-Min, G., Xiang-Jie, Y., and Meng, Z. 2008. "Microstructure Characteristics and Mechanical Properties of Rheoformed Wrought Aluminum Alloy 2024." *T. of Nonferr. Metals Soc.* 18 (6): 555-61. https://doi.org/10.2109/jcersj2.17256.

[7] Yoshida, M., Falco, S., and Todd, R. I. 2018. "Measurement and Modelling of Electrical Resistivity by Four-Terminal Method during Flash Sintering of 3YSZ." *J. Ceram. Soc. Japan* 126 (7): 579-90.

[8] Lan, R. 2020. *Electrical Resistivities of Ge-Sb-Te Alloys, Thermophys. Prop. Meas. Tech. Ge-Sb-Te Alloy. Phase Chang. Mem*. Singapore: Springer.

[9] Han, Y., Yang, W., Li, M., and Meng, C. 2019. "Comparative Study of Two Soil Conductivity Meters Based on the Principle of Current-Voltage Four-Terminal Method." *IFAC-PapersOnLine* 52: 36-42.

[10] Banhart, J. 2016. *Age Hardening of Aluminum Alloys,*

Heat Treat. Nonferrous Alloy, Heat Treating of Nonferrous Alloys, edited by Totten, G. E. ASM International.

[11] DeRose, J. A., Bałkowiec, A., Michalski, J., Suter, T., Kurzydlowski, K. J., and Schmutz, P. 2012. "Microscopic and Macroscopic Characterization of an Aerospace Aluminum Alloy (AA2024)." *Witpress* 61: 23-38.

[12] Anderson, K., Weritz, J., Kaufman, J. G., and Mackenzie, D. S. 2018. "Metallurgy of Heat Treatable Aluminum Alloys." *Alum. Sci. Technol.* 2A (11): 411-37.

[13] Staszczyk, A., Sawicki, J., and Adamczyk-Cieslak, B. 2019. "A Study of Second-Phase Precipitates and Dispersoid Particles in 2024 Aluminum Alloy after Different Aging Treatments." *Materials (Basel)* 12 (24): 4168.

[14] Styles, M. J., Hutchinson, C. R., Chen, Y., Deschamps, A., and Bastow, T. J. 2012. "The Coexistence of Two S (Al_2CuMg) Phases in Al-Cu-Mg Alloys." *Acta Materialia* 60 (12): 6940-51.

[15] Kaufman, J. G. 2019. *Properties and Applications of Wrought Aluminum Alloy, Prop. Sel. Alum. Alloy*, edited by Anderson, K., Weritz, J., and Kaufman, J. G. 202-75.

[16] Alloys, W. A. 2015. "Alloy Designations and Chemical Composition Limits for Wrought Aluminum and Wrought Aluminum Alloys."

[17] Totten, G. E., and MacKenzie, D. S. 2016. *Hardness and Electrical Conductivity Testing of Aluminum Alloys, Heat Treat. Nonferrous Alloy*, edited by Totten, G. E., and Scott MacKenzie, D. ASM Internacional.

[18] Mueller, R. A. 1967. "Relationships among the Metallurgical Condition, Hardness, and the Electrical Conductivity of Aluminum Alloys." M.Sc. thesis, The University of Missouri at Rolla.

[19] Heaney, M. B. 2004. *Electrical Conductivity and Resistivity, Electrical Measurement, Signal Processing, and Displays*, edited by Webster, J. G. Washington: CRC Press.

[20] Hintalla, W. W. 1937. "The Electrical Conductivity of the Copper-Aluminum Alloys." Bachelor theses and reports, Montana School of Mines.

[21] Boag, A., Hughes, A. E., Wilson, N. C., Torpy, A., MacRae, C. M., Glenn, A. M., and Muster, T. H. 2009. "How Complex Is the Microstructure of AA2024-T3?" *Corros. Sci.* 51 (8): 1565-8.

[22] Qin, H., Zhang, H., Sun, T. D., and Zhuang, Q. 2015. "Corrosion Behavior of the Friction-Stir-Welded Joints of 2A14-T6 Aluminum Alloy." *Int. J. Miner. Metall. Mater.* 22 (6): 627-38.

[23] Junho, O. P., Noronha, M. M. L., Mello, S. R. S., and Oliveira, C. D. 2018. "Relationship between Electrical Conductivity and the Stage of the Heat Treatments of Aging and Overaging of the Aluminum Alloy AA2024." *Mater. Sci. Forum* 930 (9): 400-4. https://doi.org/10.4028/www.scientific.net/MSF.930.400.

[24] Ives, L. K., Swartzendruber, L. J., Boettinger, W. J., Rosen, M., Ridder, S. D., Biancaniello, F. S., Reno, R. C., and Ballard, D. B. 1983. *Processing/Microstructure/Property Relationships in 2024 Aluminum Alloy Plates*. Washington: NASA.